Novel synthesis of Pd nanosheets used as highly sensitive SERS substrate for trace fluorescent dye detection

Tran Thi Bich Quyen[1]*, Doan Van Hong Thien[1], Bui Le Anh Tuan[2]

[1]*Department of Chemical Engineering, College of Technology, Can Tho University, 3/2 Street, Ninh Kieu District, Can Tho City 900000, Vietnam*
[2]*Department of Civil Engineering, Can Tho University, 3/2 Street, Ninh Kieu District, Can Tho City 900000, Vietnam*

*Corresponding author: Tel: (+84) 907 500 797; E-mail: ttbquyen@ctu.edu.vn

DOI: 10.5185/amlett.2019.2206
www.vbripress.com/aml

Abstract

In this work, a simple and effective method has been developed to synthesize Pd nanosheets that were successfully employed by reducing the Pd salt precursor in N,N-dimethylformamide (DMF), cetyltrimethylammonium bromide (CTAB) and lemon extract in the presence of Tungsten hexacarbonyl with different reaction conditions (e.g., temperature, reaction time). It indicates to be an eco-friendly, simple and novel method for the synthesis, providing a cost effective and an efficient route for the Pd nanosheets' synthesis. The Pd nanosheets were characterized by UV-vis spectroscopy, transmission electron microscopy (TEM), and X-ray diffraction (XRD). It was also demonstrated that the Pd nanosheets were both highly SERS-active and stable. Results show that Rhodamine 6G (R6G), used as a fluorescent marker, could be detected over a wide concentration range from 10^{-13} to 10^{-8} M, with the lower limit of detection being 10^{-13} M.

Keywords: Pd nanosheets (Pd NSs), environmental friendly, lemon extract, surface-enhanced raman scattering (SERS), rhodamine 6G (R6G).

Introduction

For many years ago, nanomaterials have demonstrated considerably typical properties when compared to bulk materials [**1-6]**. Furthermore, the improvement of nanotechnology and metal nanocrystals has drawn intense attention from both the scientific and industrial communities due to their common applications in plasmonics, magnetic, catalysis, electronic, and in biological medicine (i.e, drug delivery, cancer diagnosis,…) [**7-15**]. Thus, ultrathin noble metal nanosheets have recently attracted considerable attentions because of their high surface area-to-volume ratio and high density unsaturated atoms exposed on the surface, which can significantly enhance their plasmonic properties and catalytic activities [**16-22**].

Palladium (Pd) is a key constituent of many catalysts applied in industrial processes and commercial devices [**23**]. Therefore, Pd is a flexible catalyst for a large number of importantly industrial reactions such as a number of important C-C coupling reactions and hydrogenation of unsaturated organic compounds [**24-30**]. In addition, Pd nanoparticle is also a using material for sensing and hydrogen storage [**31, 32**]. For example, Pd nanowire arrays were found to be very active catalysts for ethanol oxidation for direct alcohol fuel cells [**33**]. Thus, controlling the shape of Pd nanostructures is important not only in enhancing the catalytic activity but also for other applications such as SERS, optical sensing and hydrogen storage for plasmonic sensing [**34-36**]. Besides, two-dimensional Pd nanoparticles show ferromagnetic properties that differ from those of bulk Pd, which has been reported previously [**37-39**].

Moreover, recent studies also demonstrated that the Pd nanoplates have greater capacity for hydrogen absorption and localized surface plasmon resonance (LSPR) peaks absorption in NIR regions for biological applications than bulk Pd and spherical Pd nanoparticles [**34, 40-42**]. The SERS signal intensity can be affected by electromagnetic enhancement and chemical enhancement. The electromagnetic field of light at the surface can be greatly enhanced under conditions of surface plasmon excitation; the amplification of both the incident laser field and the scattered Raman field through their interaction with the surface constitutes the electromagnetic mechanism. Chemical enhancement aims at electronic resonance and charge transfer between a molecule and a metal surface resulting in an increase in the polarizability of the molecules. In common, electromagnetic enhancement is exponential higher than chemical enhancement.

We have successful developed a novel, simple and eco-friendly approach to synthesize the Pd nanosheets using lemon extract (as a biological reducing agent),

CTAB, DMF and $W(CO)_6$ as reducing agents for Pd precursor ($Pd(acac)_2$) without using CO gas directly as the method of Huang and *et. al.* reported previously [**16**]. Herein, the Pd nanosheets' synthetic method used here is simple, cost effective, uniform particle size, environmental friendly, stable and sustainable. Because CO is an extremely toxic gas; therefore, its use and operation are quite complex. Moreover, the synthesized Pd nanosheets were also investigated the characterization and the morphology by using UV-vis, TEM and XRD.

Palladium is noble material which has surface plasmon excitation by incident light. Therefore, researches on SERS mechanisms and making new nanomaterials are great interested. The surface plasmon resonance of Pd nanosheets could be tuned by difference about the dimension and the shape of Pd nanosheets. Thus, the largest SERS enhancement could be controlled. This study shows that the Pd nanosheets may have potential applications in SERS for the detection of Rhodamine 6G (R6G) molecules due to their good stability and convenience for building "hot spots" formed by the large material's surface area.

Experimental

Materials

Palladium (II) acetylacetonate ($Pd(acac)_2$, 99%); polyvinylpyrrolidone (PVP; M_{wt} ~ 10.000); Tungsten hexacarbonyl ($W(CO)_6$; 97%) and N,N-Dimethylformamide (DMF) were purchased from Sigma-Aldrich and Merck. Cetyltrimethylammonium bromide (CTAB), aceton, and ethanol were bought from Acros. Fresh lemon (~3 months old, green shell) was purchased from a garden at Phong Dien, Can Tho City in Vietnam. All solutions were prepared using deionized water from a MilliQ system.

Methods

Preparation of lemon extract

Fresh lemon was squeezed and obtained the lemon juice mixture. After that, the lemon juice was filtered, centrifuged and washed with deioned (DI) water for three times to obtain a juice extract from lemon. This lemon aqueous extract was used for synthesis of Pd nanosheets (Pd NSs) in following steps.

Synthesis of Pd nanosheets

Palladium nanosheets (Pd NSs) were synthesized by a simple and effective approach using tungsten hexacarbonyl ($W(CO)_6$) as a reducing agent without using CO gas directly. In a typical synthesis, 60 mg of CTAB and 30 mg of PVP were dissolved in 10 mL of DMF. And then, 16 mg of $Pd(acac)_2$ and 1 mL of lemon extract were also added to 10 mL of the above DMF mixture and stirred for 20 min at room temperature. The homogeneous solution above was transferred into a 50 mL glass (flask) and 100 mg of $W(CO)_6$ be quickly added into the flask as a reducing agent for the reduction of $Pd(acac)_2$. After that, the solution was continuous stirred and heated at various temperatures and reaction times (i.e, 70 ^oC, 80 ^oC, 90^oC, 100 ^oC, and 110 ^oC; 60 min, 75 min, 90 min, and 120 min), respectively. Upon temperature and time of reaction, the reaction mixture went through a series of color changes that included light blue, blue, dark blue, and grey, etc. The solution was then centrifuged (12000 rpm; 15 min), washed with acetone to remove excess and redispersed in ethanol. The average size of the as-prepared Pd nanosheets are ~15-20 nm.

Characterization techniques and Raman measurements

The absorbance spectra of Pd nanosheet solutions were examined by UV–vis spectrophotometry (UV-675; Shimadzu). The phase structure of Pd nanosheet was determined by a X-ray diffractometer (Rigaku Dmax-B, Japan) with Cu K_α source operated at 40 kV and 100 mA. A scan rate of 0.05 deg^{-1} was used for 2θ between 10^o and 80^o. The shape and particle size of Pd nanosheets were examined by transmission electron microscope (TEM) with a Philips Tecnai F20 G2 FEI-TEM microscope (accelerating voltage 200 kV). Raman measurements were performed with a confocal Raman microscope system (Renishaw 2000). A He-Ne laser operating at λ = 532 nm was used as the excitation source with a laser power of 20 mW and 1 mW. All Raman spectra were obtained with a 10 s exposure time. The laser line was focused onto the sample in backscattering geometry using a 10× objective providing scattering areas of ca. 0.25 mm^2.

Preparation of SERS substrates

Droplets (50 μL) of Pd nanosheets (Pd NSs) of a 1.0×10^8 particles/mL nanosheets solution was spread on silicon wafers (~1 cm^2). Aqueous 10^{-8} M R6G solutions, as 5 μL droplets, was spread on the Pd NSs surfaces and kept in the dark for 1h at room temperature prior to testing. For the R6G determination, the analytes at varying concentrations (10^{-8}, 10^{-10}, 10^{-12}, and 10^{-13} M). All samples were measured under the same conditions, i.e. each sample was measured for 3 times within 10 minutes, with 3 different areas on the sample, which was focused in 10s (at 25 ^oC) to obtain SERS spectra, respectively. These measurements are reproducible with agreeable measurement errors under the same conditions.

Results and discussion

As shown in **Fig. 1**, the UV-vis spectra of Pd nanosheets (Pd NSs) exhibited with the maximum absorption peak in the NIR region from 715 nm to 865 nm – see in **Fig. 1(A)** and from 715 nm to 784 nm – see in **Fig. 1(B)**, respectively. Herein, the plasmon resonance peaks are quite match with the surface absorption of Pd nanosheets [**43**]. It is demonstrated that Pd nanosheets are created in the synthesized solution. When the reaction time of the Pd nanosheets mixture solution is increased, leading to the maximum absorption peaks also gradually shifted respective from

715 nm to 865 nm (from visible to the NIR region) due to the enhanced aspect ratio for the two-dimensional anisotropy, respectively – see in **Fig. 1(A)**. However, the reaction time is increased, leading to the intensity of absorption peaks decreased gradually – see **Fig. 1(A)**. This may be due to the solution occurs the agglomeration of nanoparticles together, resulting in the solution's color decreases gradually. Therefore, the optimal sample with reaction time at 90 min is chosen to investigate other factors in the steps following.

The absorption peak intensity is the highest at reaction temperature of 90 ºC – see in **Fig. 1(B) (d)** with the maximum absorption peak ~725 nm. When reaction temperature is lower 90 ºC or higher 90 ºC, the maximum absorption peak intensity decrease – see in **Fig. 1(B) (a-c, e, f)**, respectively. This may be due to the solution occurs the agglomeration of nanoparticles together, resulting in the solution's color decreases gradually when reaction temperature increases. And when reaction temperature is low, the reducing of Pd^{2+} ions to form the Pd nuclear occurs slow, leading to generate the Pd nanosheets decrease. Thus, the optimal sample with reaction temperature and time at 90 ºC, for 90 min is chosen to investigate other factors in the steps following.

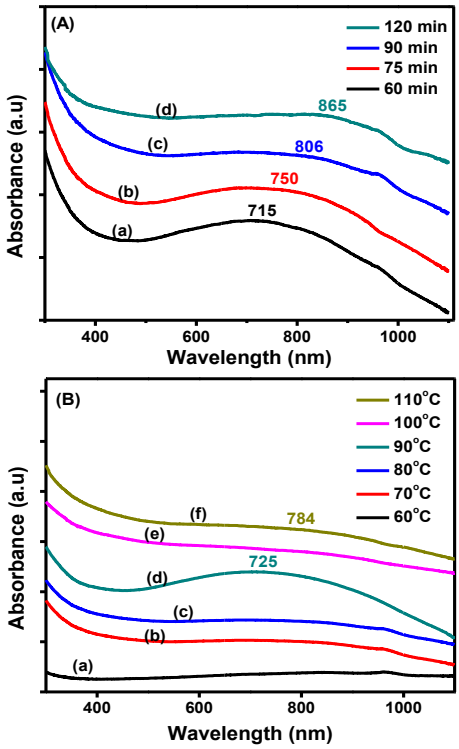

Fig. 1. UV-vis spectra of Pd nanosheets respective with various (A) Reaction times of (a) 60 min, (b) 75 min, (c) 90 min, and (d) 120 min; and (B) Reaction temperatures of (a) 60ºC, (b) 70ºC, (c) 80ºC, (d) 90 ºC, (e) 100 ºC, and f) 110 ºC.

The presence of free ions in the CTAB, lemon extract and $W(CO)_6$ have greatly accelerated for the polyol synthesis of Pd nanosheets. During the synthesis, we could easily monitor the progress of the nanosheets production through its color changes from black to light blue or dark blue, etc., due to a dramatic increase in the reduction rate of Pd ions (Pd^{2+}) to form the Pd nanosheets. The absorption intensity of synthesized samples tends to proportional increase to the Pd nanosheets' solution color. It demonstrated that the reaction rate of reducing agents using CTAB, lemon extract and $W(CO)_6$ significantly affects to particle size control of synthetic Pd nanosheets in the mixture solution.

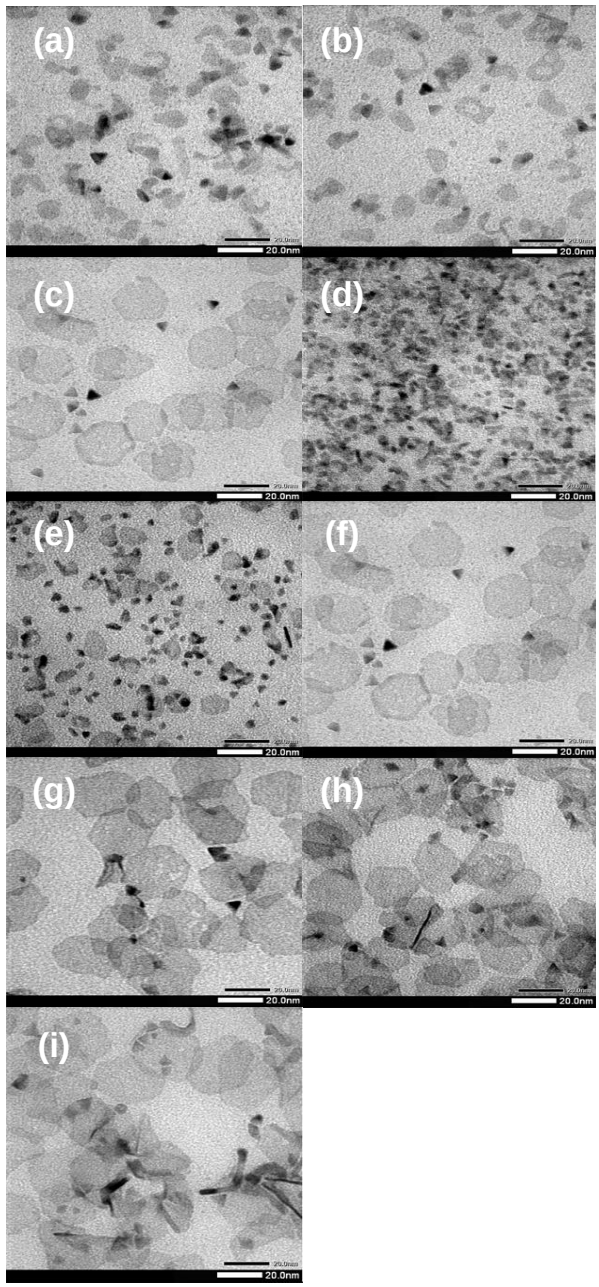

Fig. 2. TEM images of Pd nanosheets at 80 ºC with various reaction times of (a) 60 min, (b) 75 min, (c) 90 min, and (d) 120 min; and with reaction time for 90 min at different reaction temperatures of (e) 70ºC, (f) 80 ºC, (g) 90 ºC, (h) 100 ºC, and (i) 110 ºC, respectively.

Transmission electron microscopy (TEM) was used to observe the morphological and structural characterization of Pd nanosheets synthesized. **Fig. 2** shows representative TEM images of Pd nanosheets sample. From TEM images in the **Fig. 2**, most of the

nanocrystals have shape like as a hexagon profile. It is clear that each hexagonal nanosheet consists of six regular triangles. The average particle size of the Pd nanosheets are measured ~15-20 nm – see in **Fig. 2**, respectively. As shown in **Fig. 2**, the shape of Pd hexagonal nanosheets in **Fig. 2(g)** with reaction temperature at 90ºC, for 90 min obtained is clearer and more uniform than that of other samples for comparisons.

Therefore, the optimal sample with reaction condition at 90 ºC for 90 min will be chosen to synthesize Pd nanosheets for the following investigations.

The XRD pattern of palladium nanosheets is shown in the **Fig. 3**. As shown in **Fig. 3,** the characteristic peaks for Pd nanosheets appear at 2θ = 40.9º, 46.9º, 68º, 82º, and 86.5º are respectively represented the {111}, {200}, {220}, {311}, and {222} Bragg reflection. Further the XRD pattern was also compared with the JCPDS standard (No. 05-0681) and confirmed the formation of palladium nanosheets with cubic (fcc) crystal structure. This is consistent with the previously reported results [**44-46**].

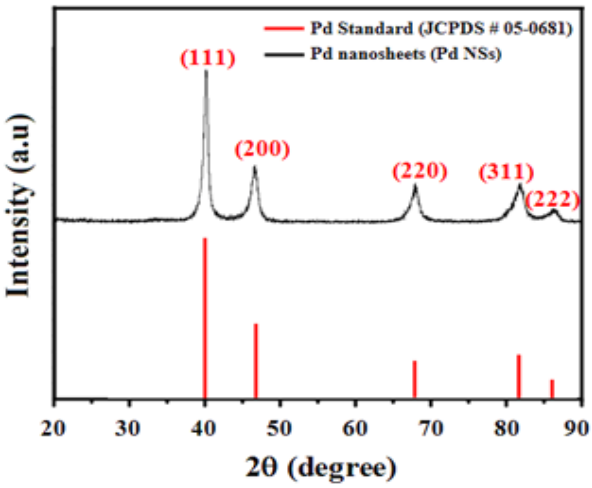

Fig. 3. XRD pattern of Pd nanosheets at 90ºC for 90 min.

Fig. 4(A) shows the SERS intensity of R6G (10^{-3} M) on the silicon substrate gave no signal, and on Pd NSs (~15-20 nm) is the highest signal using R6G (10^{-8} M). As shown in **Fig. 4(A) (b)**, the peak at ca. 777 cm^{-1} is assigned to the C–H out-of-plane bend mode. The peak at ca. 1184 cm^{-1} is assigned to the C–H in-plane bend mode. The peaks at ca. 1361, 1507, 1574 and 1652 cm^{-1} are assigned to typical aromatic ring vibrations of R6G. The enhancement factor of Pd NSs was about 10 fold-magnitude stronger than that of R6G on the silicon substrate – see **Fig. 4(A) (b, a)**, respectively. They attributed this interesting result may be due to the Pd NSs' surfaces that convenience for generation a lot of "hot-spots" at the junction between two nanosheets, increasing the electromagnetic field enhancement.

Since R6G was used as a probe molecule in SERS studies it should be very stable and without adsoption near-infrared in region. From these results, using Pd NSs to enhance SERS signals, which has been shown to be non-destructive, flexible and used to enhance intensity for the limit of detection (LOD) of R6G to the lowest concentration on the Raman signal as shown in **Fig. 4** concentration-dependent SERS spectra of R6G with typical aromatic ring vibrations, e.g., 1361, 1507, 1574 and 1652 cm^{-1}. The position of the peaks at 1361, 1507, and 1652 cm^{-1} were still detectable at the lowest R6G concentration examined 10^{-13} M.

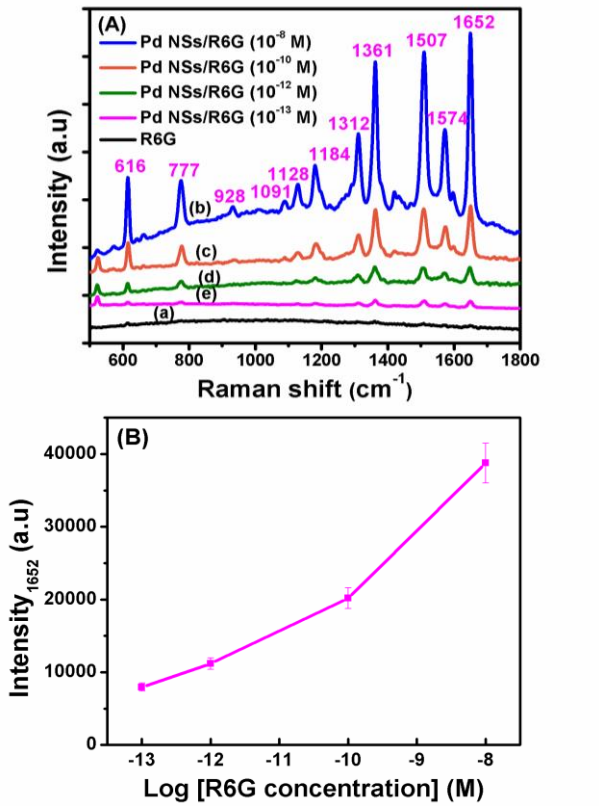

Fig. 4. (A) Representative 532 nm excited SERS spectra of (a) R6G 10^{-3} M; and with various concentrations of R6G: (b) 10^{-8} M, (c) 10^{-10} M, (d) 10^{-12} M, and (e) 10^{-13} M on Pd NSs (~15-20 nm). (B) A logarithmic plot of R6G concentration vs. signal intensity for the bands at 1652 cm^{-1}. Each data point represents the average value from three SERS spectra. Error bars show the standard deviations.

Conclusion

A simple and eco-friendly approach to synthesize the Pd nanosheets with uniform shape and small particle size have been successfully developed in this work. The using lemon extract, CTAB and $W(CO)_6$ were found to play important roles in facilitating the formation of such nanosheets. It proves to be an eco-friendly, simple and non-toxic approach when using $W(CO)_6$ and lemon extract as a biological reducing agent for the Pd nanosheets' synthesis. It indicated that synthesized Pd nanosheets have uniform, average edge length ~15-20 nm. As-prepared Pd nanosheets show an enhancement of the SERS signal due to a number of "hot spots" built by Pd nanosheets. It is also demonstrated that Pd nanosheets may have potential applications in SERS because of their good stability, low cost, and convenience for building "hot spots". Our results show that the R6G can be detected in the concentration range

10^{-8} to 10^{-13} M, with lower limit of detection (LOD) being 10^{-13} M. Therefore, Pd nanosheets could be significantly interesting in the field of plasmon-enhanced catalysis.

Acknowledgements

This research is funded by Vietnam National Foundation for Science and Technology Development (NAFOSTED) under grant number 103.99-2016.04.

References

1. Rao, C.N.R.M.; Cheetham, A.K., Eds.; *The Chemistry of Nanomaterials: Synthesis, Properties and Applications;* Wiley-VCH Verlag GmbH & Co. KgaA: Weinheim, **2004**.
2. Huang, X.; Zeng, Z.; Zhang, H., *Chem. Soc. Rev.*, **2013**, *42*, 1934. **DOI:** 10.1039/C2CS35387C
3. Zhang, H., *ACS Nano*, **2015**, *9*, 9451. **DOI:** 10.1021/acsnano.5b05040
4. Wang, Q.; O'Hare, D., *Chem. Rev.*, **2012**, *112*, 4124. **DOI:** 10.1021/cr200434v
5. Liu, H.; Du, Y.; Deng, Y.; Ye, P. D., *Chem. Soc. Rev.*, **2015**, *44*, 2732. **DOI:** 10.1039/C4CS00257A
6. Dou, L.; Wong, A.B.; Yu, Y.; Lai, M.; Kornienko, N.; Eaton, S. W.; Fu, A.; Bischak, C.G.; Ma, J.; Ding, T.; Ginsberg, N.S.; Wang, L.W.; Alivisatos, A.P.; Yang, P., *Science*, **2015,** *349*, 1518. **DOI:** 10.1126/science.aac7660
7. Sun, S.; Murray, C. B.; Weller, D.; Folks, L.; Moser, A., *Science*, **2000**, *287*, 1989. **DOI:** 10.1126/science.287.5460.1989
8. Hatzor, A.; and Weiss, P. S.; *Science*, **2001**, *291*, 1019. **DOI:** 10.1126/science.1057553
9. Eychmüller, A., *J. Phys. Chem. B*, **2000**, *104*, 6514. **DOI:** 10.1021/jp9943676
10. El-Sayed, M. A., *Acc. Chem. Res.*, **2001**, *34*, 257. **DOI:** 10.1021/ar960016n
11. Huynh, W. U.; Dittmer, J. J.; Alivisatos, A. P., *Science*, **2002**, *295*, 2425. **DOI:** 10.1126/science.1069156
12. Jariwala, D.; Sangwan, V. K.; Lauhon, L. J.; Marks, T. J.; Hersam, M. C., *Chem. Soc. Rev.*, **2013**, *42*, 2824. **DOI:** 10.1039/c2cs35335k
13. Jariwala, D.; Sangwan, V. K.; Lauhon, L. J.; Marks, T. J.; Hersam, M. C., *ACS Nano*, **2014**, *8*, 1102. **DOI:** 10.1021/nn500064s
14. Sun, Z.; Liao, T.; Dou, Y.; Hwang, S. M.; Park, M. S.; Jiang, L.; Kim, J. H.; Dou, S. X., *Nat. Commun.*, **2014**, *5*, 3813. **DOI:** 10.1038/ncomms4813
15. Quyen, T. T. B.; Chang, C. C.; Su, W. N.; Uen, Y. H.; Pan, C. J.; Liu, J. Y.; Rick, J.; Lin, K. Y.; Hwang, B. J., *J. Mater. Chem. B*, **2014**, *2*, 629. **DOI:** 10.1039/C3TB21278E
16. Huang, X.; Tang, S.; Mu, X.; Dai, Y.; Chen, G.; Zhou, Z.; Ruan, F.; Yang, Z.; and Zheng, N., *Nat. Nano*, **2011**, *6*, 28. **DOI:** 10.1038/nnano.2010.235
17. Huang, X.; Li, S.; Huang, Y.; Wu, S.; Zhou, X.; Li, S.; Gan, C. L.; Boey, F.; Mirkin, C. A.; Zhang, H., *Nat. Commun.*, **2011**, *2*, 292. **DOI:** 10.1038/ncomms1291
18. Perez-Alonso, F. J.; McCarthy, D. N.; Nierhoff, A.; Hernandez-Fernandez, P.; Strebel, C.; Stephens, I. E. L.; Nielsen, J. H.; Chorkendorff, I., *Angew. Chem. Int. Ed.*, **2012**, *51*, 4641. **DOI:** 10.1002/anie.201200586
19. Saleem, F.; Zhang, Z.; Xu, B.; Xu, X.; He, P.; Wang, X., *J. Am. Chem. Soc.*, **2013**, *135*, 18304. **DOI:** 10.1021/ja4101968
20. Duan, H.; Yan, N.; Yu, R.; Chang, C. R.; Zhou, G.; Hu, H. S.; Rong, H.; Niu, Z.; Mao, J.; Asakura, H.; Tanaka, T.; Dyson, P. J.; Li, J.; Li, Y., *Nat. Commun.*, **2014**, *5*, 3093. **DOI:** 10.1038/ncomms4093
21. Yin, X.; Liu, X.; Pan, Y. T.; Walsh, K. A.; Yang, H., *Nano Lett.*, **2014**, *14*, 7188. **DOI:** 10.1021/nl503879a
22. Hong, J.W.; Kim, Y.; Wi, D.H.; Lee, S.; Lee, S.U.; Lee, Y.W.; Choi, S. I.; Han, S. W., *Angew. Chem. Int. Ed.*, **2016**, *55*, 2753. **DOI:** 10.1002/anie.201510460
23. Roucoux, A.; Schulz, J.; Patin, H., *Chem. Rev.*, **2002**, *102*, 3757. **DOI:** 10.1021/cr010350j
24. Li, Y.; Hong, X. M.; Collard, D. M.; El-Sayed, M. A., *Org. Lett.*, **2000**, *2*, 2385. **DOI:** 10.1021/ol0061687
25. Reetz, M. T.; E. W. Dipl.-Chem., *Angew. Chem. Int. Ed.*, **2000**, *39*, 165. **DOI:** 10.1002/(SICI)1521-3773(20000103)39**:**1<165**::**AID-ANIE165>3.0.CO;2-B
26. Franzén, R., *Canadian J. Chem.*, **2000**, *78*, 957. **DOI:** 10.1139/v00-089
27. Son, S. U.; Jang, Y.; Park, J.; Na, H. B.; Park, H. M.; Yun, H. J.; Lee, J.; Hyeon, T., *J. Am. Chem. Soc.*, **2004**, *126*, 5026. **DOI:** 10.1021/ja039757r
28. Astruc, D.; *Inorg. Chem.*, **2007**, *46*, 1884. **DOI:** 10.1021/ic062183h
29. Berhault, G.; Bisson, L.; Thomazeau, C.; Verdon, C.; Uzio, D., *Appl. Catal. A.*, **2007**, *327*, 32. **DOI:** 10.1016/j.apcata.2007.04.028
30. Redjala, T.; Remita, H.; Apostolescu, G.; Mostafavi, M.; Thomazeau, C.; Uzio, D., *Oil Gas Sci. Technol. Rev. IFP*, **2006**, *61*, 789. **DOI:** 10.2516/ogst**:** 2006019
31. Tobiška, P.; Hugon, O.; Trouillet, A.; Gagnaire, H., *Sens. Actuator B- Chem.*, **2001**, *74*, 168. **DOI:** 10.1016/S0925-4005(00)00728-0
32. Hübert, T.; Boon-Brett, L.; Black, G.; Banach, U., *Sens. Actuator B-Chem.*, **2011**, *157*, 329. **DOI:** 10.1016/j.snb.2011.04.070
33. Xu, C. W.; Wang, H.; Shen, P. K.; Jiang, S. P., *Adv. Mater.*, **2007**, *19*, 4256. **DOI:** 10.1002/adma.200602911
34. Xiong, Y.; McLellan, J. M.; Chen, J.; Yin, Y.; Li, Z. Y.; Xia, Y., *J. Am. Chem. Soc.*, **2005**, *127*, 17118. **DOI:** 10.1021/ja056498s
35. Li, Y.; Lu, G.; Wu, X.; Shi, G., *J. Phys. Chem. B*, **2006**, *110*, 24585. **DOI:** 10.1021/jp0638787
36. Langhammer, C.; Zorić, I.; Kasemo, B.; Clemens, B. M., *Nano Lett.*, **2007**, *7*, 3122. **DOI:** 10.1021/nl071664a
37. Bouarab, S.; Demangeat, C.; Mokrani, A.; Dreyssé, H., *Phys. Lett. A*, **1990**, *151*, 103. **DOI:** 10.1016/0375-9601(90)90857-K
38. Mendoza, D.; Morales, F.; Escudero, R.; Walter, J., *J. Phys. Condens. Matter*, **1999**, *11*, 317. **DOI:** 10.1088/0953-8984/11/28/101
39. Suzuki, I. S. S. M.; Walter, J., *Phys. Rev. B*, **2000**, *62*, 14171. **DOI:** 10.1103/PhysRevB.62.14171
40. Kishore, S.; Nelson, J. A.; Adair, J. H.; Eklund, P. C., *J. Alloy. Comp.*, **2005**, *389*, 234. **DOI:** 10.1016/j.jallcom.2004.06.105
41. Xiong, Y.; Chen, J.; Wiley, B.; Xia, Y.; Yin, Y.; Li, Z. Y., *Nano Lett.*, **2005**, *5*, 1237. **DOI:** 10.1021/nl0508826
42. Xiong, Y.; Wiley, B.; Chen, J.; Li, Z. Y.; Yin, Y.; Xia, Y., *Angew. Chem. Int. Ed.*, **2005**, *44*, 7913. **DOI:** 10.1002/anie.200502722
43. Kooij, E. S.; Ahmed, W.; Zandvliet, H. J. W.; Poelsema, B., *J. Phys. Chem. C*, **2011**, *115*, 10321. **DOI:** 10.1021/jp112085s
44. Sathishkumar, K. S. a. Y. S. M., *Int. J. Mater. Sci.*, **2009**, *4*, 11. **DOI:** 228083693_Palladium_Nanocrystal_Synthesis_Using_ Curcuma_longa_Tuber_Extract
45. Yang, X.; Li, Q.; Wang, H.; Huang, J.; Lin, L.; Wang, W.; Sun, D.; Su, Y.; Opiyo, J. B.; Hong, L.; Wang, Y.; He, N.; Jia, L., *J. Nanopart. Res.*, **2010**, *12*, 1589. **DOI:** 10.1007/s11051-009-9675-1
46. Bankar, A.; Joshi, B.; Kumar, A. R.; Zinjarde, S., *Mater. Lett.*, **2010**, *64*, 1951. **DOI:** 10.1016/j.matlet.2010.06.021

